International Journal of Multiphysics
Volume 18, No. 4, 2024
ISSN: 1750-9548

Fabrication and Characterization of Polysulfone-Graphene Oxide Mixed Matrix Membranes for Reduction Permeability and Selectivity of CO2, N2, CH4 Gases

Rohallah Bakhshi[1], Mostafa Keshavarz Moravaji[2, *], Arsalan Parvareh[3]

[1]Department chemical engineering, Borujerd Branch, Islamic Azad University, Borujerd,Iran
[2]Department of Chemical Engineering, Amirkabir University of Technology (Tehran Polytechnic), Tehran,Iran
[3]Chemical Engineering and petroleum faculty, Razi university, Kermanshah,Iran
*Corresponding author

Abstract

Reduced graphene oxide is fabricated from graphite oxidation through a modified Hummer method. The polysulfone fabricated by a phase separation method. Different amounts of graphene oxide (0.0, 0.25 and 0.5 wt.% of polymer) were used. After preparation of the membranes, the cross-sectional structure and their upper surface were assessed by scanning electron microscopy (SEM) and the surface roughness of the membranes was assessed by atomic force microscopy (AFM). From SEM, an increase in the concentration of graphene oxide in the polymer matrix resulted in a thicker sponge layer and disappearance of the finger-like cavities. From the gas permeation test, by addition of 0.25% graphene oxide to the polymer matrix, CO_2 permeability was increased from 62 GPU to 77 GPU, while addition of 0.5 wt.% resulted in a lower permeability (69.55 GPU). Nitrogen gas permeation flux of membranes decreased from 10.93 GPU to 4 GPU by addition of 0.50 wt.% of graphene oxide. Methane gas permeation flux is reduced from 11.5 GPU to 7 GPU and 4.92 GPU by addition of 0.25% and 0.50% graphene oxide, respectively. and CO2/N2 selectivity for all three membrane samples: 5.8, 12.3 and 17.9 respectively. And CO2/CH4 selectivity was obtained: 5.43, 10.95 and 14.2.

Keywords: Membrane gas separation; Mixed matrix membrane; Graphene oxide

Introduction

Applying polymeric membranes for the gas separation is a major concern among researchers. Limitations and drawbacks like the low thermal and chemical resistance and the swelling of polymeric membranes have made researchers modify the structure of membranes applied in the gas separation processes.

Inorganic membranes are able to withstand high temperature and are durable compared to the polymer membranes. Researchers seek to find methods to achieve the benefits of both polymeric and inorganic membranes in a simultaneous manner. Mixed membrane matrixes (MMM) that have been fabricated prevail over the restriction and drawbacks of both membranes. To fabricate MMMs, inorganic fillers are applied in the polymer membrane matrix. In recent years, MMMs have been used for different applications like the gas separation, water desalinization, heavy metals removal from water, gas absorption and discharges.

Graphene, known as a low permeability filler, has not been weighed in the construction of MMMs for the separation of gas. Natural graphene is an inert substance and due to its ability to propagate in the solvents and reaction being very low, it does not form a homogeneous mixture with the polymer. In order to increase the stability of graphene in solvents and form a bond with the polymer chain, introducing application groups on the graphene surface is essential. it is a graphene-based nanoparticle, and is linked to oxygen-bound groups. Active cell groups, like carboxyl and hydroxyl in graphene oxide, can propagate in the polymer matrix in a proper manner which can improve the membrane gas separation properties [1, 2].

Applying graphene oxide for the MMM fabrication, creates a pathway for small gas molecules to pass but prevents the large gas molecules passing [3, 4].

Recent studies have shown, the nanoparticles of graphene oxide in the structure of the membranes increased the mechanical and thermal durability of the membranes [5-9].

Researchers have addedgraphene oxide to the structure of the polysulfide hollow fiber membrane, and therefore, the tensile strength and length stretching increased during the membrane breakage by 36.3 % and 8.79 % respectively [10].

It is also observed that the graphene polyculture-oxide mixed matrix membrane has a high thermal stability and its mechanical properties have increased when 0.25 % of graphene oxide was added to the matrix [11].

Mr Ruiwen and colleagues, the synergistic effect of Nipc and RGO with excellent physical interface provides lower charge transfer resistance and better charge storage capacity [34].

Jiliang and colleagues have also had high efficiency in a work by adding RGO on the natural silk bed to revive the produced materials [35].

According to the latest studies, Reduced graphene oxide is rarely applied in improving the structure of polymeric membranes for the nitrogen/carbon dioxide/methane separation. In this study, polysulfone MMMs were prepared by applying graphene oxide as a filler additive. After assessing the structure and specifications of the membranes, they were applied in the nitrogen/carbon dioxide/methane gas separation. In this work, by reducing graphene oxide, these oxidized functional groups are removed to obtain graphene material. By coating this material on polysulfone polymer, because it has high mechanical properties, high stability, good electrical and thermal conductivity, and a high surface-to-volume ratio, it increases work efficiency for separation.

Experiments

Primitive materials

The membrane (Psd Used P-3550, Chemicals Amco, USA) is applied as the base polymer for the membrane fabrication. The reason for selecting this polymer is its good mechanical stability and easy processing [12-15]. The N-methyl-acetamide solvents of (DMAC> 95%) and tetrahydrofuran (THF≥ 99.5%) were procured from the Merck, and used as the solvents. Natural graphene sheets (≤ 20 µm), ethanol and (KMnO4) were purchased from Aldrich. (H_2SO_4, 95-97 wt. %), (HCl) and (H_2O_2, 30 wt. %) were catered from Merck, Germany. Distilled water was made in the laboratory and utilized as the coagulant in the process of fabricating membranes.

Synthesis of graphene oxide

The oxidation of graphite was applied to prepare graphene oxide by the modified Hummer method [3, 16].

Here, 3 gr of powder graphite was dissolved in 100 ml of H_2SO_4; the solution mingled in an ice bath at 0 °C; 10 gr of potassium permanganate was added to the solution in a slow manner and the solution was stirred at below 10 °C for 3 hours. The temperature was increased to 40 °C and the solution was stirred for 35 minutes in a vigorous manner. 150 ml of distilled water was added to the solution and it was heated to about 100 °C where it was riled for 20 minutes at this temperature. Then 500 ml of distilled water and 15 ml of hydrogen peroxide were added to the solution. The solution was placed on an ultrasonic apparatus for 1 hour in order to separate the large graphene oxide grains. The mixture was filtered and then rinsed by distilled water containing 3 vol % of sulfuric acid to remove metal ions. The produced graphene oxide was dried in an oven for 8 hours and then was grinded to obtain a graphene oxide powder**.**

Preparing the polymer solutions

In order to fabricate MMMs, three types of the polymer solutions were prepared as follows:

The first solution was free of graphen oxide, where the solution contained polysulfone polymer (30 wt %), dimethyl acetamide (35 wt %), tetrahydrofuran (30 wt %) and ethanol (5 wt %). The ratios related to the polymer solutions are given elsewhere [12, 17-18].

To prepare 100 g of this solution, first, 35 g of the DMAC solution was poured into a glass bottle and 30 g of tetrahydrofuran was added. When the mixture of solvents in the bottle was being stirred by a mechanical riler, 30 g of polymer was gradually added to the solvent. The gradual addition of the polymer prevents the agglomeration of the polymer seeds. The solution was riled for 24 hours to dissolve all the polymer in the solvent. After making sure that all polymer seeds in the solvent were dissolved, 5 g of ethanol was added to it and riled again for 2 hours to achieve a homogeneous solution. To remove the air bubbls in it, the solution was placed on an ultrasonic apparatus for 60 minute and then kept at ambient temperature for 1 day.

The second solution was prepared using graphene oxide by 0.25 % (w/w) of the polymer. To prepare 100 g of this solution, 35 g of dimethyl acetamide was first poured into a glass bottle, then graphene oxide was added to the dimethyl acetamide solution. The bottle containing the solution was placed on an ultrasonic apparatus for 1 hour so that the particles will be dispersed in the solvent. For the better dispersion of graphene oxide particles in the solution of DMAc, the suspension solution was placed on a sonicator micro-tip (505 watts, 3 s) for 5 minutes. Then 30 g of the tetrahydrofuran solvent was added to the solution and it was stirred mechanically for 60 minute. 30 g of polysulfone was gradually added to this solution and the resulted solution was stirred for 24 hours to dissolve all the polymer in this solution. Finally, 5 g of ethanol was added to it and the bottle of the solution was placed on an ultrasonic apparatus for 1 hour to discharge the air bubbles. To make sure that all air bubbles in the polymer solution were discharged, the solution was placed at ambient temperature for 24 hours before use.

The preparation of the third solution was similar to the second one, but the polymer solution was prepared using graphene oxide at a rate of 0.5 % (w/w) of the polymer. The proportional compositions of the prepared solutions are shown in Table 1.

Before applying the prepared polymer solutions to fabricate the membrane, the viscosity of solutions was measured by a viscometer.

Table 1. Proportional composition of materials in the polymer solution

Solution name	Polymer (wt %)	DMAC (wt %)	THF (wt %)	Ethanol (wt %)	RGO (wt% of polymer)
S_1	30	35	30	5	0
S_2	30	35	30	5	0.25
S_3	30	35	30	5	0.5

Membrane construction via a phase separation method

To make the membranes, the polymer solution was spread on a glass sheet and was strewn as a film with a balanced thickness. The solution was kept on the sheet for 120 seconds to reach to a membrane with a dense skin. Then the plate was plunged in a container full of distilled water at ambient temperature to accomplish the phase separation process. The fabricated membrane was spilled from the glass sheet and kept in distilled water for 1 day to sweep the remaining kosher. Then the flat membrane sheet was dried at ambient temperature.

Specification of the synthesized graphene oxide

2.5.1. Transmission Electron Microscopy (TEM)

The structure of the synthesized graphene oxide surface was distinguished through (TEM, Zeiss EM900, Germany). For this purpose, a small amount of graphene oxide was poured into ethanol and the solution was placed on an ultrasonic device for 60 minute to disperse graphene oxide into the ethanol. The resulting suspension was kept at the environment temperature for 15 minutes. Then some of the resulted solution was placed into the microscope to capture an image of the graphene oxide structure.

Fourier Transform Infrared Spectroscopy (FTIR)

The chemical structure of graphene oxide was analyzed by FTIR spectroscopy. For this purpose, the samples were placed in a dryer at 60 °C overnight to allow the excess water to be discharged. The samples were then grinded along with potassium bromide at the ratio of 1:10.

characterization of the fabricated MMM

Scanning Electron Microscopy (TEM)

To display cross-sectional and surface images of the fabricated membranes, sthe caning electron microscopy (TM3000, HITACHI, Japan) was used. Small pieces of 5 × 5 cm membranes were cut in liquid nitrogen, so that the cross-sectional structure would break with no failure. The broken parts were placed in an oven at 60 °C and for 2 hours for the removal of moisture from the membranes pores. The membrane samples were then coated with platinum to enhance the reflectivity of electrons shifted by the scanning electron microscope and to provide better quality images.

Atomic Force Microscopy (AFM)

To assess the membrane surface roughness and determine the average roughness (Ra), the atomic force microscopy (AFM, SPA-300 HV, Seiko, Japan) was applied. For this purpose, small pieces of 5 × 5 cm membranes were cut and the surface roughness was assessed by AFM.

Mechanical stability of the membranes

The extra length and rigidity tensile at breaking point of the MMM were measured by ASTM D3930 through a tensile test machine (LRX 2 Llyod SKN). For this purpose, membranes were cut to pieces of 6 cm in length and placed in the device.

Differential Scanning Calorimetry (DSC)

The transition temperature (Tg) of the produced MMM was delineated by a scanning differential calorimeter model (DSC, Mettler Toledo DSC, 822e). The samples were heated about 30°C to 410°C at an intensity of 11 °C/min, after which the cooling took place in the reverse manner. The heating and cooling operation was run twice: the first was to calibrate the sample and the second was to determine Tg.

Thermal Gravimetric Analysis (TGA)

The thermal stability analysis of grapheme oxide and the prepared membranes were conducted through a thermal gravimetric analyser (TGA, Perkin Elmer). The sample was heated until a change in its weight was observed. The sample was heated within 32 °C to 805 °C at intensity of 12 °C/min at 25 ml/min of the flow rate of nitrogen.

Membrane gas separation test

The separation performance of the membranes for carbon dioxide, nitrogen and methane gases was conducted through a gas permeability apparatus. A circular piece of the membrane impressive surface zone of 13 cm² was placed in a stainless steel module. The gas was injected to the module at 24 °C and 5 bar pressure. Using a soap bubble flow meter, the gas permeability flux of the membranes was measured. The gas permeation flux (P/L) was calculated through Eq. (1) [19]:

$$P / L = Q / (A.\Delta P) \qquad (1)$$

P is the flux of the gas permeability (cm^3/s), A is the effective surface of the membrane (cm^2), ΔP is the pressure difference between the two sides of the membrane (cmHg), L is the thickness of the membrane (cm) and Q is the permeated gas flow (cm^3/s).

The ideal selectivity, α_{ij}, is given as [20]:

$$\alpha_{ij} = P_i / P_j \quad (2)$$

according to the following performance equation:

$$\alpha_{ij} = (D_i/D_j) * (k_i/k_j) \quad (3)$$

The D_i/D_j ratio is the ratio of the penetration coefficients of two gases and can be called kinetic selectivity. which expresses the different sizes of two gases, the K_i/K_j ratio is the ratio of the absorption coefficients of the two gases and it can be called adsorption selectivity, which expresses the relative condensability of two gases. So membrane selectivity is a function of two factors, kinetic selectivity and adsorption selectivity. In the gas separation process, the selectivity of the membrane strongly depends on whether the membrane-forming polymer is high or low temperature it depends on the glass transfer.

The apparatus is showing in Fig. (1).

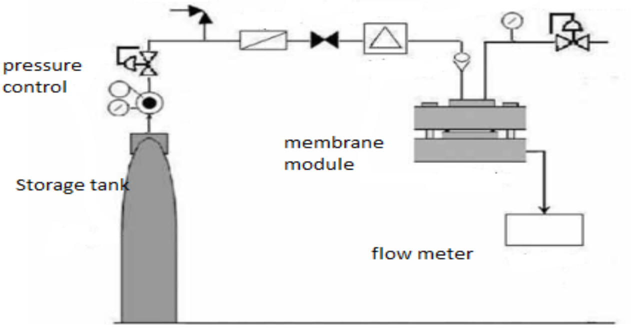

Figure 1: Schematic of the testing apparatus

Results and discussion

Structure and specifications of the synthesized graphene oxide

The TEM images of the synthesized graphene oxide with various magnifications are displayed in Figure 2. The TEM image indicates that graphene oxide was synthesized through a smooth and transparent manufacturing process.

The FTIR of Reduced graphene oxide and spectrum of graphite are shown in Figure 3.

There is no significant peak in the graphite spectrum, while the presence of various types of oxygenating agents in graphene oxide was confirmed by the IR spectrum.

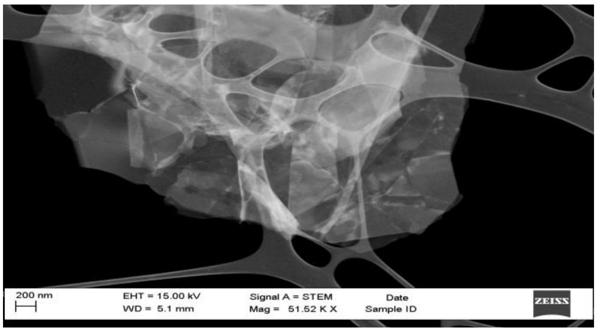

Figure 2. TEM picture of the synthesized graphene oxide.

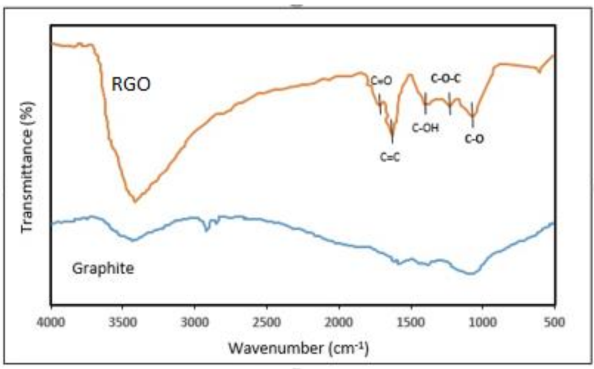

Figure 3. FTIR spectra of graphite and Reduced graphene oxide.

For Reduced graphene oxide at the spectra between 3000 (cm^{-1}) and 3700 (cm^{-1}), an absorption band is expanded, which is related to the stretching vibrations of the O-H group on the surface or the water molecules absorbed in the layer's graphene oxide. This absorption band includes several stretching O-H states indicating the functional groups of O-H being present in the form of alcohol, phenol, or carboxylic acid at the surface of graphene oxide [21, 22].

Two couriers, appeared at 1735 cm^{-1} and 1605 cm^{-1}, could be the tensile vibrations related to the double bond of hydrocarbons.

The thermal degradation of graphene oxide is related to the functional groups connected to the surface. The first weight loss at 120 % occurred at the temperature of 125 °C which was related to the removal of water in graphene oxide [23]. The second weight loss occurred within 120 °C and 255 °C, at a rate of 27.5 %, which was due to the removal of oxygen in the agent group [24].

The third weight loss occurred within 245 °C and 855 °C, due to removal more oxygen stable residues in manufacture main RGO, pyrolysis the unstable carbon- RGO structure [8, 25].

The general weight loss of 59 % occurred at 950 °C. The TGA analysis revealed that graphene oxide had more thermal instability than natural graphite, indicating that graphene oxide was successfully synthesized.

Morphology of the Surface of the prepared membranes

The morphology of the surface of the fabricated membranes was analyzed through an atomic microscopy force (Figure 4).

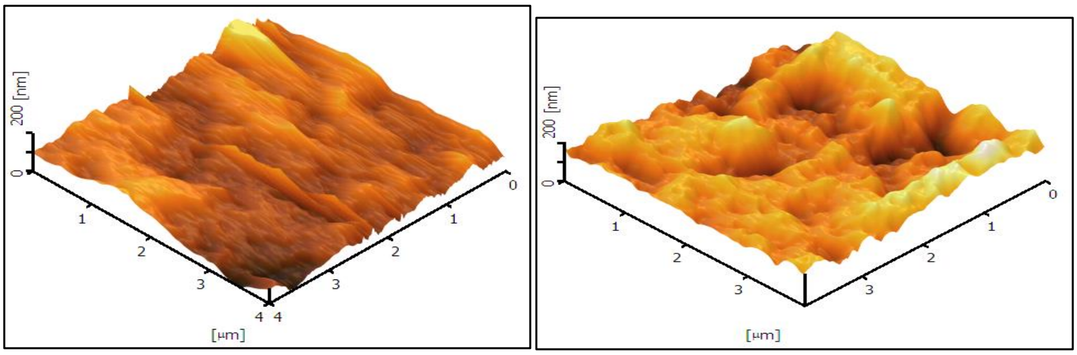

Figure 4. AFM images of the membrane surface, ((A) 0.24 wt % of RGO and (B) 0.52 wt % of RGO.

Table 2. Average surface roughness of the membranes

Membrane name	RGO (wt %)	Mean roughness Ra(nm)
M_1	0	13
M_2	0.25	14.5
M_3	0.5	18

Moreover, the increment of the roughness of the membrane surface can be attributed to the growth of the exchange rate of solvent/non-solvent during the phase separation process just the hydrophilic nature the RGO [4, 6]. Changing the solvent may result in the formation of polymer spheres or nodes, which results in a mild surface roughness of the membrane. This can lead to the development of the membrane porosity.

Structural morphology of the prepared membranes

The scanning electron microscopy was used to evaluate the cross-sectional structure of the membranes and the images are shown in Fig. (5).

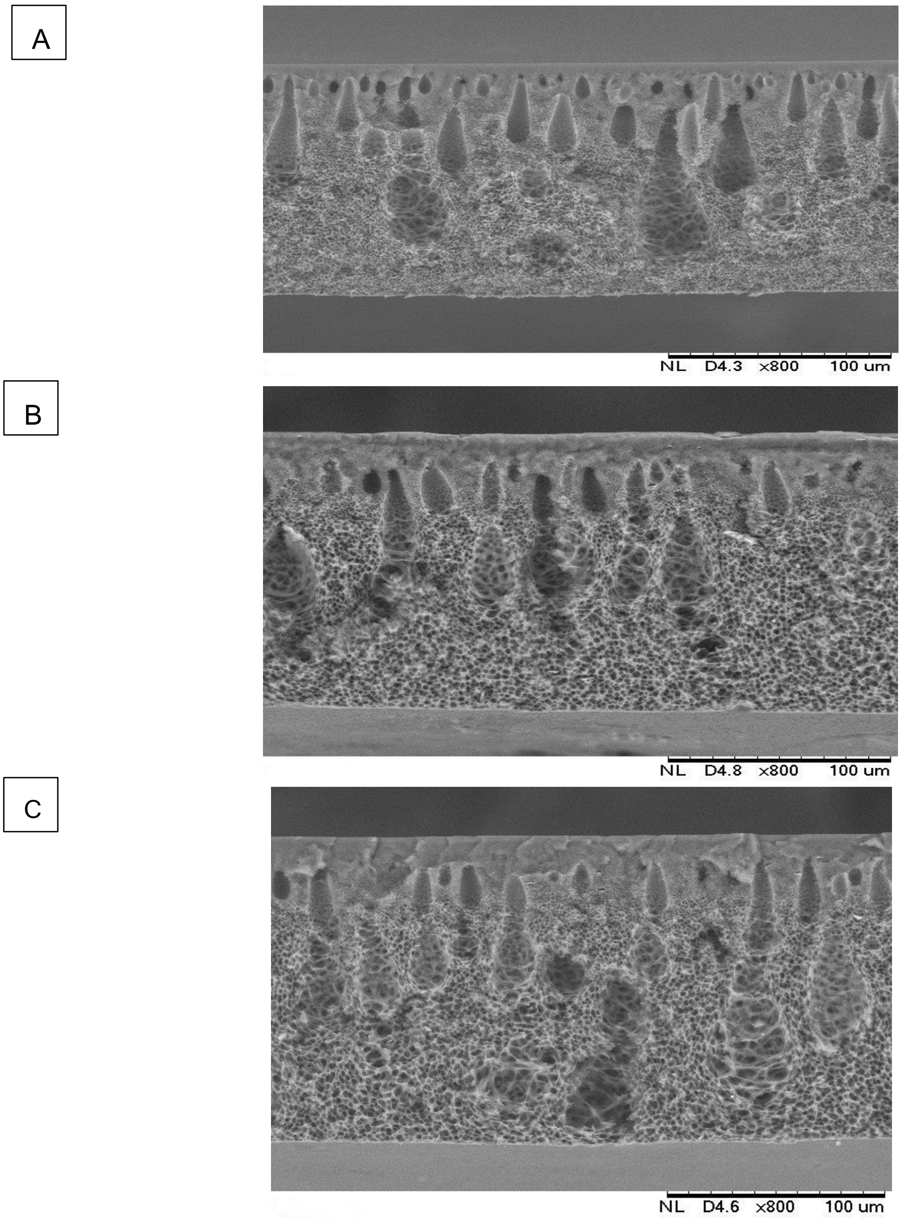

Figure 5. SEM cross-sectional images of the prepared membranes (A) Pure polysulfide; (B) 0.25 wt. % RGO; and (C) 0.50 wt. % RGO

From images, the apt membranes showed an asymmetric structure, which consists of a dense active skin with a thin sponge-like substrate and a thick fuzzy layer with large cavities. Using 2 min air gap time before the immersion of the membrane in the gelation bath, causes the evaporation of THF resulting in the formation of a selective thin layer on the membrane surface [17].

Moreover, the foundation of the spongy and finger-like structure during the wet phase separation process is pertinent to exchange solvents (DMAc, THF, Etoh), and insoluble (water) contained in coagulation bath. In general, when the rate of the phase separation process is high, the possibility of the structure being in the form of the insoluble truck is high, like when a dactyl structure is formed, whereas the formation of the sponge-like structure is related to a low rate of the phase separation [26].

Gas separation performance of the prepared MMMs

The gas permeation in the membranes for carbon dioxide, nitrogen, and methane at the constant pressure of 5 bar and 24 °C are measured and results are display in Figure 10. The flux of carbon dioxide increased, while the nitrogen and methane gas permeation decreased. The obtained results indicated that the MMMs with 0.25 % (M2) and 0.5 % (M3) of graphene oxide have 24.2 % and 13.6 % higher carbon dioxide permeation flux respectively, the Nitrogen permeation flux in M2 and M3 membranes decreased 76 % and 179.5 % respectively. In addition, the methane permeation flux in M2 and M3 membranes decreased by 62.7 % and 129.9 % respectively.

As it is observed, the flux reduction of nitrogen was higher than that of methane gas. The ideal solubility of nitrogen gas is reported to be much lower than that of carbon dioxide [31].

Observed SEM images that the skin layer of the pure membrane was thicker and has more pores compared to the MMMs.

It is proved that π-π grains existing in graphene oxide tend to be highly polarized [10].

The permeation flux of the carbon dioxide gas increased by adding 0.25 % of graphene oxide to the polymer matrix. the thickness of the selected layer relatively decreased. Thickening of the density of the selected layer prevents the carbon dioxide passing and decreases the permeability.

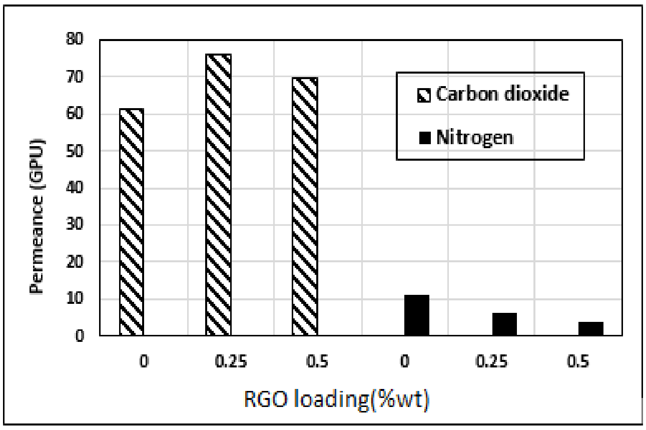

Figure 6. Permeability of carbon dioxide, nitrogen and methane

As it is observed in Figure 6, the permeability flux of carbon dioxide was 62 GPU for the pure membrane, which reached to 77 GPU by adding 0.25 % of graphene oxide to the polymer matrix. The addition of 0.5 % of graphene oxide resulted in the flux reduction to 70 GPU. An increase in the concentration of graphene oxide up to 0.5 % resulted in the reduction of the carbon dioxide permeation flux,

The N_2 flux permeation is lower than that of carbon dioxide, where it was 10.93 GPU for the pure membrane and 4 GPU for the membrane fabricated with 0.5 % of graphene oxide. The methane gas permeation flux was 12 GPU for the pure membrane and reached 7 GPU and 5 GPU for the membranes fabricated with 0.25 % and 0.5 % of graphene oxide respectively. The carbon dioxide selectivity of the prepared membranes is shown in Figure 7.

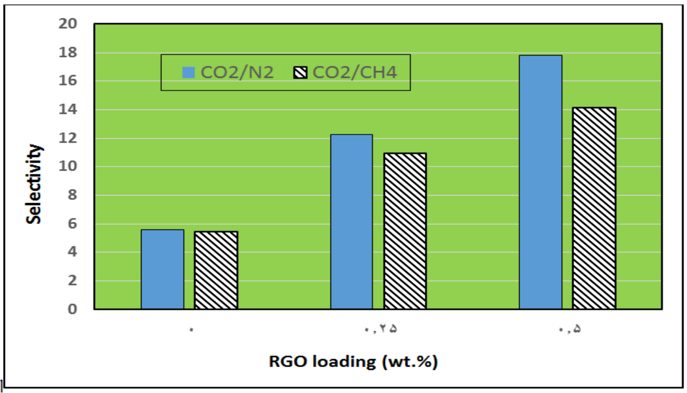

Figure 7. CO_2 selectivity in relation to N_2 and CH_4

An increase in the concentration of graphene oxide increased the CO_2 selectivity of the membranes. In the explanation of the results of the membrane surface images it was explained that by adding graphene oxide to the polymer solution, a thin layer of the dense layer was formed. The inert gas molecules like nitrogen did not pass, which resulted in the improvement of the membrane selectivity. According to Figure 8, the amounts of carbon dioxide selectivity for nitrogen are 5.8, 12.3 and 17.9 respectively. The amounts of carbon dioxide selectivity for methane were 5.43, 10.95 and 14.2 respectively. The permeability and selectivity results are given in Table 3,4:

Table 3. Permeability CO_2, N_2, CH_4

Components	RGO without	RGO
CO_2	62	77
N_2	10.93	4
CH_4	12	7

Table 4. Selectivity CO_2/N_2 , CO_2/CH_4

Component	M1	M2	M3
CO2/N2	5.8	12.3	17.9
CO2/CH4	5.43	10.95	14.2

According to the carbon dioxide and nitrogen separation performance of the fabricated membranes, it can be deduced that adding graphene oxide to the polymer matrix improves the carbon dioxide permeation flux. Applying graphene oxide with the concentration of 0.25 % by weight in the polymer matrix can optimize the membrane structure, which cosequently increased the carbon dioxide permeation flux with a good selectivity compared to that of methane.

The gas permeation results obtained in the present study are compared with a number of published results and display in Table 5.

As it is observed, the fabricated membrane with 0.25 % of graphene oxide exhibited a better performance for the separation of carbon dioxide and nitrogen.

Table 5. Gas flux permeation.

Membrane type	**Polymer**	**Filler**	**CO_2 Permeance (GPU)**	**N_2 Permeance (GPU)**	**Reference**
Flat sheet[a]	Polysulfone	functionalized carbon nano-fiber (CNF)	5.1	2.2	[32]

Flat sheet[b]	Polysulfone	--------	23	1.45	[33]
Flat sheet[c]	Polysulfone	C15A 2.0%	76	17.75	[13]
Flat sheet[c]	Polysulfone	RGO (0.25 wt. %)	76.04	6.21	This study

[a] P =2 bar at ambient temperature
[b] P = 4.48 bar feed pressure at ambient temperature
[c] P = 5 bar feed pressure and T= 25 ^{o}C

Conclusion

In the present study, three polysulfone solutions were prepared by the addition of graphene oxide (0.0, 0.25 and 0.05 % (w/w)). The membranes were fabricated through a phase separation process. The addition of 0.25 % of graphene oxide to the polymer solution, caused the thickness of the selected layer to reduce from 132 nm to 86 nm. However, the increase of graphene oxide up to 0.50 % increased the selected layer thickness to 102 nm. The permeability CO_2 in the best form was 77GPU. The N_2 permeation was lower than that of carbon dioxide, where it was 4 GPU. The methane gas permeation flux was 7. For M1, M2 and M3 membranes, the carbon dioxide selectivity's versus nitrogen were 5.8, 12.3 and 17.79 respectively. Carbon dioxide gas selectivity's versus methane for M1, M2 and M3 membranes were 5.43, 10.95 and 14.2 respectively. An important factor in the separation of carbon dioxide, nitrogen and methane molecules is their molecular size.

REFERENCES

[1] Kuila T, Bose S, Mishra AK, Khanra P, Kim NH, Lee JH. Chemical functionalization of graphene and its applications. Progress in Materials Science. 2012 Sep 1;57(7):1061-105.

[2] Yang X, Wang X, Yang J, Li J, Wan L. Functionalization of graphene using trimethoxysilanes and its reinforcement on polypropylene nanocomposites. Chemical Physics Letters. 2013 May 10;570:125-31.

[3] Li X, Cheng Y, Zhang H, Wang S, Jiang Z, Guo R, Wu H. Efficient CO2 capture by functionalized graphene oxide nanosheets as fillers to fabricate multi-permselective mixed matrix membranes. ACS applied materials & interfaces. 2015 Mar 11;7(9):5528-37.

[4] Checchetto R, Miotello A, Nicolais L, Carotenuto G. Gas transport through nanocomposite membrane composed by polyethylene with dispersed graphite nanoplatelets. Journal of membrane science. 2014 Aug 1;463:196-204.

[5] Liu H, Huang W, Yang X, Dai K, Zheng G, Liu C, Shen C, Yan X, Guo J, Guo Z. Organic vapor sensing behaviors of conductive thermoplastic polyurethane–graphene nanocomposites. Journal of Materials Chemistry C. 2016; 4(20): 4459 - 69.

[6] Ganesh BM, Isloor AM, Ismail AF. Enhanced hydrophilicity and salt rejection study of graphene oxide-polysulfone mixed matrix membrane. Desalination. 2013 Mar 15; 313:199-207.

[7]Yadav M, Rhee KY, Park SJ. Synthesis and characterization of graphene oxide/ carboxymethy lcellulose / alginate composite blend films. Carbohydrate polymers. 2014 Sep 22;110:18-25.

[8] Wang Y, He Q, Qu H, Zhang X, Guo J, Zhu J, Zhao G, Colorado HA, Yu J, Sun L, Bhana S. Magnetic graphene oxide nanocomposites: nanoparticles growth mechanism and property analysis. Journal of Materials Chemistry C. 2014; 2(44):9478-88.

[9] Liu H, Li Y, Dai K, Zheng G, Liu C, Shen C, Yan X, Guo J, Guo Z. Electrically conductive thermoplastic elastomer nanocomposites at ultralow graphene loading levels for strain sensor applications. Journal of Materials Chemistry C. 2016;4(1):157-66.

[10] Zhao L, Cheng C, Chen YF, Wang T, Du CH, Wu LG. Enhancement on the permeation performance of polyimide mixed matrix membranes by incorporation of graphene oxide with different oxidation degrees. Polymers for Advanced Technologies. 2015 Apr;26(4):330-7.

[11] Ionita M, Pandele AM, Crica L, Pilan L. Improving the thermal and mechanical properties of polysulfone by incorporation of graphene oxide. Composites Part B: Engineering. 2014 Mar 1;59:133-9.

[12] Zulhairun AK, Ng BC, Ismail AF, Murali RS, Abdullah MS. Production of mixed matrix hollow fiber membrane for CO2/CH4 separation. Separation and Purification Technology. 2014 Nov 24;137:1-2.

[13] Zulhairun AK, Ismail AF, Matsuura T, Abdullah MS, Mustafa A. Asymmetric mixed matrix membrane incorporating organically modified clay particle for gas separation. Chemical Engineering Journal. 2014 Apr 1;241:495-503.

[14] Zulhairun AK, Ismail AF. The role of layered silicate loadings and their dispersion states on the gas separation performance of mixed matrix membrane. Journal of Membrane Science. 2014 Oct 15;468:20-30.

[15] Kim S, Chen L, Johnson JK, Marand E. Polysulfone and functionalized carbon nanotube mixed matrix membranes for gas separation: theory and experiment. Journal of Membrane Science. 2007 May 15;294(1-2):147-58.

[16] Zhao Y, Ding H, Zhong Q. Preparation and characterization of aminated graphite oxide for CO2 capture. Applied Surface Science. 2012 Mar 1;258(10):4301-7.

[17] Nordin NA, Ismail AF, Racha SM, Cheer NB, Bilad MR, Putra ZA, Wirzal MD. Limitation in fabricating PSf/ZIF-8 hollow fiber membrane for CO2/CH4 separation. Indonesian Journal of Science and Technology. 2018;3(2):138-49.

[18] Nordin NA, Ismail AF, Mustafa A, Murali RS, Matsuura T. The impact of ZIF-8 particle size and heat treatment on CO 2/CH 4 separation using asymmetric mixed matrix membrane. RSC Advances. 2014;4(94):52530-41.

[19] Shen J, Zhang M, Liu G, Guan K, Jin W. Size effects of graphene oxide on mixed matrix membranes for CO2 separation. AIChE Journal. 2016 Aug;62(8):2843-52.

[20] Zahri K, Wong KC, Goh PS, Ismail AF. Graphene oxide/polysulfone hollow fiber mixed matrix membranes for gas separation. RSC advances. 2016;6(92):89130-9.

[21] Mahmoud KA, Mansoor B, Mansour A, Khraisheh M. Functional graphene nanosheets: The next generation membranes for water desalination. Desalination. 2015 Jan 15;356:208-25.

[22] Chang DW, Choi HJ, Jeon IY, Seo JM, Dai L, Baek JB. Solvent-free mechanochemical reduction of graphene oxide. Carbon. 2014 Oct 1;77:501-7..

[23] Wu T, Wang X, Qiu H, Gao J, Wang W, Liu Y. Graphene oxide reduced and modified by soft nanoparticles and its catalysis of the Knoevenagel condensation. Journal of Materials Chemistry. 2012;22(11):4772-9.

[24] THI VU TH, THI TRAN TT, THI LE HN, THI NGUYEN PH, Bui NQ, Essayem N. A new green approach for the reduction of graphene oxide nanosheets using caffeine. Bulletin of Materials Science. 2015 Jun;38:667-71.

[25] Loryuenyong V, Totepvimarn K, Eimburanapravat P, Boonchompoo W, Buasri A. Preparation and characterization of reduced graphene oxide sheets via water based exfoliation and reduction methods. Advances in Materials Science and Engineering. 2013; 2013(1): 923403.

[26] Rahbari-Sisakht M, Ismail AF, Rana D, Matsuura T. A novel surface modified polyvinylidene fluoride hollow fiber membrane contactor for CO2 absorption. Journal of membrane science. 2012 Oct 1;415:221-8.

[27] Lan Y, Liu H, Cao X, Zhao S, Dai K, Yan X, Zheng G, Liu C, Shen C, Guo Z. Electrically conductive thermoplastic polyurethane/polypropylene nanocomposites with selectively distributed graphene. Polymer. 2016 Aug 5;97:11-9..

[28] Kiran SA, Thuyavan YL, Arthanareeswaran G, Matsuura T, Ismail AF. Impact of graphene oxide embedded polyethersulfone membranes for the effective treatment of distillery effluent. Chemical Engineering Journal. 2016 Feb 15;286:528-37..

[29] Nwanonenyi SC, Obidiegwu MU, Onuegbu GC. Effects of particle sizes, filler contents and compatibilization on the properties of linear low density polyethylene filled periwinkle shell powder. International journal of Engineering and Science. 2013;2(2):1-8.

[30] Hashemifard SA, Ismail AF, Matsuura T. Mixed matrix membrane incorporated with large pore size halloysite nanotubes (HNTs) as filler for gas separation: Morphological diagram. Chemical Engineering Journal. 2011 Aug 1;172(1):581-90.

[31Baker RW. Membrane technology and applications. John Wiley & Sons; 2023 Dec 18..

[32] Kiadehi AD, Jahanshahi M, Rahimpour A, Ghoreyshi SA. The effect of functionalized carbon nano-fiber (CNF) on gas separation performance of polysulfone (PSf) membranes. Chemical Engineering and Processing: Process Intensification. 2015 Apr 1;90:41-8..

[33] Junaidi MU, Leo CP, Kamal SN, Ahmad AL, Chew TL. Carbon dioxide removal from methane by using polysulfone/ SAPO-44 mixed matrix membranes. Fuel processing technology. 2013 Aug 1;112:1-6

[34] Meyyappan M, Sunkara MK. Inorganic nanowires: applications, properties, and characterization. CRC Press; 2018 Sep 3.

[35] Wang XM, Bo L, Zhu M, Jie T, Guo L, Wang J, Wang Y, Hu J. Geochemical Behavior of Rare Earth Elements in Mining-Affected Waters, Southwest China. Southwest China.